



Mapping cyanobacterial blooms in Lake Champlain's Missisquoi Bay using QuickBird and MERIS satellite data

Sarah M. Wheeler^a, Leslie A. Morrissey^{a,*}, Suzanne N. Levine^a, Gerald P. Livingston^a, Warwick F. Vincent^b

^a Rubenstein School of Environment and Natural Resources, University of Vermont, Burlington VT 05405, USA

^b Dépt de biologie & Centre d'études nordiques (CEN), Université Laval, Québec City, QC, Canada, G1V 0A6

ARTICLE INFO

Article history:

Received 6 October 2010

Accepted 4 May 2011

Available online 22 July 2011

Communicated by Timothy Mihuc

Keywords:

Cyanobacteria

QuickBird

MERIS

Chlorophyll

Phycocyanin

Blooms

ABSTRACT

C-phycocyanin (C-PC) and chlorophyll-*a* (Chl-*a*) concentrations for the eutrophic waters of Missisquoi Bay, Lake Champlain (VT–QC) were retrieved from Envisat's MERIS radiance data (300 m spatial resolution) and validated against coincident georeferenced transect observations. Pigment concentrations were also predicted from empirically calibrated QuickBird data (2.4 m spatial resolution) using selected band ratios and principal components analysis. The QuickBird NIR/Red band ratio accounted for approximately 80% of the variability in observed Chl-*a* concentration, allowing for detailed mapping of phytoplankton spatial distributions. C-PC concentrations, in contrast, were somewhat poorly modeled ($R^2 = 0.68$). Use of these data for monitoring purposes, however, is also limited by the need for coincident field observations. Chl-*a* concentrations were also accurately retrieved from the MERIS data (Mean Relative Error = -0.6%) despite high concentrations of suspended particles and dissolved organic matter in the bay waters. C-PC concentrations were underestimated on average by 2.1%, but by 10–20% at high C-PC concentrations ($\geq 80 \mu\text{g/L}$) and as the proportion of cyanobacteria in the phytoplankton community decreased. The relatively high overall accuracies observed, however, attest to the robustness of the MERIS semi-analytical retrieval algorithms used to quantify potentially toxic cyanobacteria cell densities without the need for coincident field data. Our analyses over a 17 day period captured the peak and collapse of a late summer cyanobacterial bloom, illustrating the value of remote sensing to provide synoptic and timely information on the abundance and distribution of cyanobacterial populations that, in turn, can facilitate public health risk assessment.

© 2011 International Association for Great Lakes Research. Published by Elsevier B.V. All rights reserved.

Introduction

Cyanobacterial blooms worldwide impact freshwater habitats, drinking water quality, recreational use of lake waters, and, if toxic, pose a threat to animal and human health (Downing et al., 2001; Falconer, 2001; Hunter et al., 2009). Particularly vulnerable are small to moderately-sized temperate waters where seasonally warm temperatures and excess nutrient concentrations due to cultural eutrophication often favor cyanobacterial growth. Missisquoi Bay on the Vermont–Québec border in northern Lake Champlain is typical of many such waters, where episodic and often toxic cyanobacterial blooms have severely restricted municipal and recreational use of bay waters in recent years (LCBP, 2010).

Charged with assessing the potential impacts and health risks associated with cyanobacterial blooms, water quality and public health managers have long relied on conventional point sampling approaches combined with laboratory analyses to differentiate between nuisance and potentially toxic blooms. Point sampling

efforts, however, are inherently and severely limited in their ability to represent the patchy and dynamic distribution of phytoplankton (Kutser, 2004; Moses et al., 2009; Rantajarvi et al., 1998). Facing increasing population demands on surface waters, changing land use, limited budgets, and a changing climate that favors cyanobacterial growth, there is a clear need for improved monitoring systems to evaluate water quality and public health risk assessment on local to regional scales.

Airborne and satellite remote sensing offer great promise to complement in situ water quality monitoring efforts in inland waters by providing synoptic and periodic spectral measures of pigment concentrations indicative of algal and cyanobacterial abundance (Gitelson et al., 2000). The spatial and temporal context provided by these data, in turn, can aid risk assessment and ecological modeling, as well as direct sampling efforts to improve the cost effectiveness of field programs. Perceived uncertainties regarding the utility of remote sensing in small to moderate-sized inland waters, data availability, technical requirements, and cost, however, have greatly hindered the integration of remote sensing into current water quality monitoring programs.

Unlike in oceanic waters, the optical properties of inland waters are rarely dominated by the absorption and backscattering of incident

* Corresponding author at: Rubenstein School of Environment and Natural Resources, University of Vermont, Burlington, VT 05405, USA. Tel.: +1 802 656 2695.

E-mail address: Leslie.Morrissey@uvm.edu (L.A. Morrissey).

light by photoactive pigments, such as chlorophyll-*a* (Chl-*a*), that are closely linked to phytoplankton abundance. Instead, water color is largely determined by colored dissolved organic matter (CDOM) and suspended inorganic particulates, neither of which co-vary with phytoplankton biomass (Gitelson et al., 2000; Moses et al., 2009). Algorithms to derive pigment concentration from spectral data in inland waters, therefore, must take advantage of well recognized absorption and reflectance features in the red and near infrared (NIR) wavelengths that are sensitive to Chl-*a* concentration, but relatively insensitive to other optically active constituents in the water column (Gitelson et al., 2000; Gons et al., 2002; Moses et al., 2009).

Because all phytoplankton contain Chl-*a*, measures of its concentration alone cannot be used to map the abundance and distribution of cyanobacterial blooms in mixed assemblages. Cyanobacteria, however, are the only freshwater group that also possess the blue chlorophyll accessory pigment C-phycoyanin (C-PC) in relatively high concentrations, which allows light energy for photosynthesis to be efficiently captured even in turbid waters (Reynolds, 1984; Vincent, 2009). C-PC has a strong absorption feature near 620 nm (Dekker et al., 1992). Spectral returns from waters dominated by cyanobacteria, therefore, are distinct from those dominated by eukaryotic algae and can be used to effectively map the presence and abundance of cyanobacterial populations (Becker et al., 2009; Jupp et al., 1994; Ruiz-Verdú et al., 2008; Simis et al., 2005).

Empirical approaches for estimating Chl-*a* and C-PC concentrations have been widely employed in freshwater systems using broadband medium spatial resolution (20–30 m) sensors, such as Landsat TM, ETM and SPOT (e.g., Chang et al., 2004; Mayo et al., 1995; Torbick et al., 2008; Vincent et al., 2004). Higher spatial resolution sensors, such as DigitalGlobe's QuickBird (2.4 m), offer promise of even more detailed information on phytoplankton abundance and distribution to aid understanding and modeling of the processes involved in the formation and propagation of blooms. The use of empirical models with these data, however, require calibrating observed pixel radiance in specific spectral bands or band derivatives to coincident in situ Chl-*a* concentration measurements. In addition, the regression models used to estimate pigment concentration are limited in application to the location and acquisition date of the data from which they are derived (Matthews et al., 2010).

In contrast, physically-based, semi-analytical algorithms in combination with narrow-bandwidth spectral data can retrieve Chl-*a* and C-PC concentrations directly without the need for coincident field observations, as has been well demonstrated in both coastal and freshwater systems using experimental, e.g. HYPERION (Brando and Dekker, 2003; Jupp et al., 1994; Koponen et al., 2001; Kutser, 2004; Pierson and Strombeck, 2001), and ocean color sensors, e.g. MODIS (Becker et al., 2009; Moses et al., 2009; Pan et al., 2010; Reinart and Kutser, 2006) and MERIS (Doerffer and Schiller, 2007; Gons et al., 2008; Schroeder et al., 2007; Simis et al., 2005).

Integration of remote sensing into water quality monitoring programs in inland waters is severely hindered by the paucity of airborne or satellite sensors designed for this purpose. At present, the European Space Agency's Medium Resolution Imaging Spectrometer (MERIS) onboard the ENVISAT satellite offers narrow bandwidth data positioned near pigment absorption maxima that, in conjunction with bio-optical models, can be used to retrieve Chl-*a* and C-PC concentrations indicative of phytoplankton and cyanobacterial biomass (e.g. Hunter et al., 2009; Matthews et al., 2010). The relatively coarse spatial resolution (300 m) of this sensor, however, limits its application in freshwater systems to only the largest of these waters (Hunter et al., 2008a; Kutser et al., 2006).

We report here our evaluation of the potential of remote sensing to support public health risk assessment and water quality monitoring activities in Missisquoi Bay in northern Lake Champlain, by providing synoptic and multi-temporal information on the abundance and distribution of potentially toxic cyanobacteria. Our specific objectives

were (1) to evaluate the utility of ENVISAT's MERIS to quantify Chl-*a* and C-PC concentrations over time, and (2) assess the utility of MERIS and QuickBird imagery to map the spatial heterogeneity of the cyanobacterial blooms in the bay.

Methods

Study area

Located on the Vermont–Québec border (Fig. 1), Missisquoi Bay (45.039° N, 73.128° W) is a shallow (mean depth = 2.8 m), eutrophic embayment 77.5 km² in area that has experienced toxic cyanobacterial blooms over the past decade (Mihuc et al., 2006; Mihuc et al., 2005). Increasingly declining water quality and severe restrictions on recreational and municipal use of bay waters has impacted the local economy and focused public, state, and provincial attention on water quality and watershed management concerns (LCBP, 2002, LCBP, 2010; Missisquoi Bay Inter-Agency Advisory Committee –Montérégie, 2004; U.S. EPA, 2002).

Three tributaries drain the 3100 km² Missisquoi watershed, the Missisquoi River from the south, the Rock River from the east and the Pike River from the north. Like many inland waters in the Northeast, Missisquoi Bay suffers from excess phosphorus inputs from agricultural and urban runoff, in addition to a substantial internal supply from sediments (Smeltzer, 2003).

Cyanobacteria have always been present in Lake Champlain's phytoplankton community, although recent assessments indicate a transition towards a more eutrophic community with *Microcystis* replacing *Anabaena* as the most common taxon in Missisquoi Bay (Mihuc et al., 2008; Watzin et al., 2006). Both genera are capable of producing cyanotoxins, although their presence in bay waters was only first documented in 1999. Since then, the observed concentration of hepatotoxic microcystins in Missisquoi Bay waters has often exceeded the WHO guideline (1 µg/L) for safe drinking water (Missisquoi Bay Inter-Agency Advisory Committee –Montérégie, 2004).

Satellite observations

QuickBird high spatial resolution (2.4 m) satellite imagery acquired 17 August 2004 over Missisquoi Bay was procured from DigitalGlobe, Inc. The data represent measured radiance in four relatively wide (~100 nm) spectral bands in the visible (B, G, R) and near-infrared (NIR) (Table 1). The 1:4800 orthorectified imagery was delivered in VT SPCS NAD 83 as digital number (DN) values.

Two MERIS images were also acquired from the European Space Agency (ESA) over Lake Champlain on 24 August and 3 September 2004

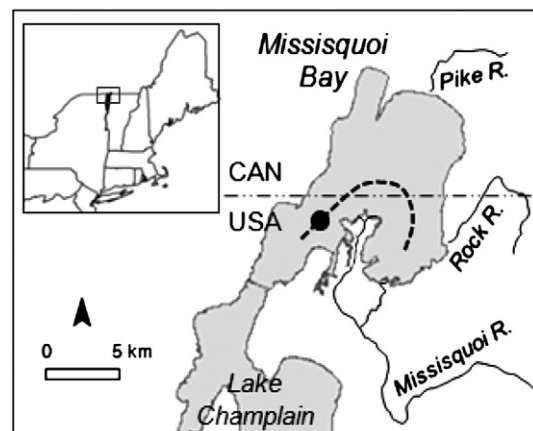


Fig. 1. Northern Lake Champlain showing field transect (---) and VTDEC monitoring site (●) (1992 – present) locations within Missisquoi Bay.

Table 1
Satellite sensor specifications.

	QuickBird	MERIS
Spatial resolution (Pixel size)	2.4 m	300 m
Visible Bands (B,G,R)	3	8
Near infrared bands	1	7
Bandwidth (nm)	60–140	7.5–20
Scene size (km)	16.5 × 16.5	575 × 575
Revisit capability	1–3.5 days	2–4 days

(Table 1). MERIS's fifteen narrow (~10 nm) spectral bands are ideally positioned for retrieval of both Chl-*a* and C-PC concentrations in turbid, eutrophic waters. Spatial resolution of the Level 1B full resolution data was 300 m. The MERIS imagery was delivered as geolocated, top-of-atmosphere calibrated radiance values ($W/m^2/sr/\mu m$).

Field observations

In vivo fluorescence of Chl-*a* and C-PC was measured continuously along georeferenced field transects coincident with satellite observations to characterize the phytoplankton spatial distributions. Data were collected within ± 1 h of both the QuickBird and MERIS satellite overpass. Transects ranged in length between approximately 4–10 km. Water was collected ahead of the bow wave of a boat traveling about 1.9 m/s (~3.6 kts) from a depth of 10 cm and pumped sequentially through a Turner® A 10 flow-through fluorometer fitted with a phycocyanin kit (excitation wavelength: 620 nm; emission detection wavelength: 650 nm), a Wetlab® mini chlorophyll fluorometer, and a Wetlab® transmissometer, before being expelled off the boat's stern. The tubing through which the water was pumped was wrapped with black tape to avoid phytoplankton light shock. Data from all instruments, as well as time, location and speed, were recorded at 10-second intervals using a Campbell Scientific® data logger synchronized with a Garmin® GPSMAP76 receiver.

At quasi-random locations along each transect, water samples were collected in duplicate for subsequent laboratory analysis. Water samples also were collected at the beginning and end of each transect for subsequent analysis of optical properties. Phytoplankton samples were preserved with acid Lugol's solution and all samples were stored in darkened insulated containers for transport back to the laboratory. Two vertical profiles were collected each sampling day (to 2 m depth) to determine phytoplankton distribution throughout the water column. Light extinction rates were evaluated in association with each profile at 0.5 m intervals using a LI-COR® submersible light meter.

Laboratory analyses

Water samples collected in the field were returned to the laboratory within five hours of collection. Aliquots supporting pigment, optical property and total suspended sediment analyses were filtered through GF/F filters and immediately stored at -23 °C. Chl-*a* and C-PC concentrations were determined spectrophotometrically. Chl-*a* was extracted using hot ethanol and analyzed, with pheophytin correction, using a Shimadzu UV-1602 spectrophotometer as described by Sartory and Grobbelaar (1984). C-PC extraction was conducted using a multiple disruption method in which the cells were burst open using glycerol, distilled water and a tissue grinder (Quesada and Vincent, 1999). The extracted supernatant was analyzed at 562 nm, 615 nm and 652 nm using a Shimadzu UV-1601 spectrophotometer and C-PC concentrations estimated using equations from Wyman and Fay (1986). The extraction-based concentrations of Chl-*a* and C-PC were then used to calibrate the fluorescence field data using linear regression.

To assess the contributions of other optically active constituents influencing reflectance at the water's surface, we measured the optical density of the CDOM and suspended inorganic particles relative to the total absorption at 620 nm and 665 nm, i.e. at those wavelengths at which C-PC and Chl-*a* respectively are known to strongly absorb. The optical density of the total particulate matter was analyzed using a Cary 300 dual-beam spectrophotometer and integrating sphere. Dissolved organic matter was analyzed using the same spectrophotometer on water filtered through a 0.20 μm sodium acetate filter and stored at 3 °C.

Phytoplankton community composition was evaluated by direct count. The phytoplankton were concentrated in settling chambers and counted to genus level under an Olympus IX70 inverted microscope at 40 \times . Ten fields were assessed yielding several hundred cell counts per analysis.

Satellite data preprocessing

QuickBird satellite data were converted from DN values to water-leaving radiances ($W/m^2/sr/\mu m$) using DigitalGlobe's coefficients and the equations described in Krause (2003). No atmospheric correction was applied. Conditions at the time of acquisition were clear and dry, and the minimum radiances observed in the red and NIR spectral bands indicated little atmospheric contribution. To further preserve the integrity of the spectral measurements, the data were not destriped, although banding in the blue and red spectral bands was evident.

Pixels representing land and near shore areas where reflectance from shoreline vegetation, bottom sediments, or submerged macrophytes could potentially confound analyses were masked using a NIR band threshold to restrict analyses to the open-water areas of the bay. The image was then resampled using a 3 \times 3 pixel mean kernel to eliminate possible misregistration between the transect observations and the image. Pixel size of the resultant image was 7.2 m. The field transect locations were then overlain onto the imagery and the radiance values associated with each sample point extracted.

MERIS image preprocessing included correction for atmospheric attenuation, radiance conversion, and projection of the data. The imagery was corrected for Rayleigh scattering, ozone and water vapor absorption (Rahman and Dedieu, 1994) using the Simplified Method for Atmospheric Correction (SMAC) processor incorporated into the BEAM VISAT software (Fomferra and Brockmann, 2006) to retrieve the water leaving radiance reflectance ($mW/m^2/sr/nm$). The imagery was then projected to UTM Zone 18N WGS84 using the BEAM VISAT software.

A MERIS NIR band 12 (779 nm) threshold was used to mask pixels representing land or near shore areas. Individual pixels exhibiting sunglint, cloud cover, or processing errors were also screened based on quality control data provided with the imagery. The open water area of the bay was represented by approximately 650 pixels in the resultant images.

MERIS pixel radiances along the field transect were extracted and the field measured Chl-*a* and C-PC concentrations averaged to their corresponding pixels. As a result, each MERIS-derived concentration along the transect was validated against the average of at least 16 field observations.

Retrieval of pigment concentrations

Chl-*a* and C-PC concentrations were retrieved using MERIS spectral bands centered at 620, 665, 709, and 779 nm and the semi-analytical algorithms developed by Gons et al. (2005) and Simis et al. (2005) respectively. Detailed evaluation of both algorithms is given in Ruiz-Verdú et al. (2008) and Hunter et al. (2010). Absorption in the 620 and 665 nm bands is assumed to be dominated by water and phytoplankton pigments (C-PC and Chl-*a* at 620 nm, and Chl-*a* alone

at 665 nm), whereas absorption at 709 nm and 779 nm is assumed to be dominated by water alone. The Gons algorithm predicts Chl-*a* concentration using a NIR:Red band ratio corrected for absorption by water and total backscatter (Gons et al., 2002; Gons et al., 2005). The Simis C-PC algorithm also corrects for water and total backscatter, as well as Chl-*a* absorption at 620 nm (Simis et al., 2005; Simis et al., 2007). Absorption by CDOM and suspended particles was neglected following Simis et al. (2005) to limit the number of optically active constituents modeled.

The accuracy of the MERIS-retrieved pigment concentrations was evaluated in comparison to the spatially-averaged measured concentrations acquired along each field transect. Differences between the predicted and field observed concentrations are reported as the mean relative error, expressed in percent: $MRE = (\text{predicted} - \text{observed}) / \text{observed}$.

QuickBird spectral data were used to predict Chl-*a* and C-PC concentrations by regressing single band, band ratios, and derived principal components against the field transect concentration data. The band ratios tested were derived from the NIR/Red and the (Blue-Red)/Green spectral bands following Yacobi et al. (1995) and Mayo et al. (1995) respectively. The principal component analysis (PCA) followed Chacon-Torres et al. (1992). The simplest model with the highest coefficient of determination (R^2) was then applied to the entire QuickBird image to predict pigment concentrations throughout the bay.

ERDAS Imagine (Leica, 2009) and ArcGIS (ESRI, 2010) were used to analyze the satellite imagery and co-register the field transect data. Statistical analyses were performed using SAS (SAS, 2010).

Results

Field observations

Over the period of study (August 17 through September 03, 2004), cyanobacteria dominated the phytoplankton communities in Missisquoi Bay, representing on average 73–89% of the total phytoplankton biovolume (Table 2). Chlorophytes (4–19%) and Cryptomonas (5–8%) represented the remaining fraction. *Microcystis aeruginosa* dominated the assemblages on each sampling date. In vivo PC:Chl-*a* ratios averaged over each sampling date ranged from 1.1 to 2.4 which is consistent with observations from cyanobacterial blooms in northern European eutrophic lakes (Hunter et al., 2008b; Ruiz-Verdú et al., 2008; Simis et al., 2005).

Field observations on August 17th indicated an extensive but spatially variable cyanobacterial bloom across much of Missisquoi Bay. Phytoplankton populations sampled along the eastern section of the transect were often concentrated as surface scums, whereas in the more windswept western section, they were relatively evenly distributed throughout the upper meter of the water column. Chl-*a* and C-PC concentrations along the transect averaged 95.7 and 105.1 $\mu\text{g/L}$ respectively (Table 2), but varied greatly over the length of the transect (Fig. 2). Overall, Chl-*a* concentrations ranged from 38 to 157 $\mu\text{g/L}$, but in general, were highest in the protected waters represented by the eastern section of the transect (kilometers 0–4) and lowest near the center of the bay. Elevated Chl-*a* concentrations

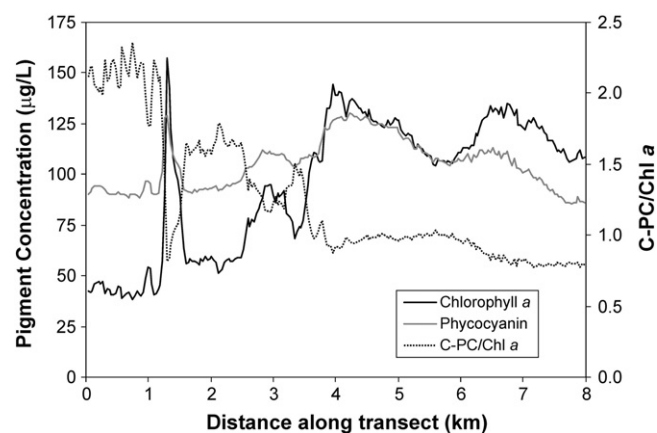


Fig. 2. Pigment concentrations ($\mu\text{g/L}$) observed along an 8 km transect in Missisquoi Bay on August 17th, 2004. Observations were made traveling from east to west, i.e. from right to left as plotted.

were also observed along the frontal boundaries where the Missisquoi River waters entered the bay (e.g., kilometer 1.3). C-PC concentrations ranged from 85.5 to 130.4 $\mu\text{g/L}$, tracking the variability in Chl-*a* concentration ($R^2 = 0.88$), but displaying no clear trend. As a consequence, C-PC:Chl-*a* ratios varied greatly over the length of the transect, ranging from 0.8 to 1.0 in the most productive areas and 1.2–2.3 elsewhere (Fig. 2). Patch size, as measured by the distance between local minima in Chl-*a* concentrations, ranged in scale from decameters to kilometers.

Optical data

Table 3 summarizes the results of the optical depth measurements for Missisquoi Bay on August 17th. Not surprising given the shallow depth of the bay and the moderate wind speeds observed (Table 2), total suspended solids (TSS) were an important constituent of the water column, averaging $14.2 \pm 6.2 \mu\text{g/L}$. Suspended inorganic particles and CDOM together accounted for 68% of the total absorption at 620 nm and nearly 60% at 665 nm, emphasizing the challenge for pigment retrieval algorithms in these turbid waters.

QuickBird regression analyses

Observed Chl-*a* concentrations along the August 17th transect were best modeled using the QuickBird NIR/Red band ratio ($R^2 = 0.75$; Fig. 3; Table 4). Principal component analysis indicated that 98.3% of the variability in the data was accounted for by the first two principal components and that much of the banding information was contained in components 3 and 4. Regression of principal components 1 and 2 alone against observed Chl-*a* concentrations, however, showed no improvement over the N-IR/Red ratio. C-PC concentrations, in contrast, were somewhat poorly modeled regardless of band or band combination examined. Lacking a spectral band positioned near the 620 nm C-PC absorption maximum, prediction of

Table 2
Summary of field transect observations on each sampling date.

Date	Satellite sensor	Wind speed/direction ^a	Chl <i>a</i> ^b (Mean \pm 1SD)	C-Phycocyanin ^b (Mean \pm 1SD)	n	% Biovolume ^c			Dominant Taxon (% Biomass)
						CY	CH	C	
17 Aug. 2004	QuickBird	14.0 SSW	95.7 \pm 32.7	105.1 \pm 12.4	234	89	4	7	<i>Microcystis aeruginosa</i> (CY 66%) <i>Anabaena flos-aquae</i> (CY 20%)
24 Aug. 2004	MERIS	8.1 NNW	58.1 \pm 8.5	98.5 \pm 14.4	112	73	19	8	<i>Microcystis aeruginosa</i> (CY 67%) <i>Ulothrix</i> (CH 16%)
3 Sept. 2004	MERIS	17.7 S	15.9 \pm 1.4	37.8 \pm 4.1	167	84	11	5	<i>Microcystis aeruginosa</i> (CY 75%) <i>Coelosphaerium</i> (CY 10%)

^a Wind speed (km/h) and direction recorded at Colchester Reef (Vermont Monitoring Cooperative, 2004).

^b Reported as $\mu\text{g/L}$.

^c Taxon: cyanobacteria (CY), chlorophyta (CH), and Cryptomonas (C).

Table 3
Measured optical variables for Missisquoi Bay (Mean \pm 1SD).

Optical Variable	Wavelength (λ)	Absorption coefficient
a_{water}^a		0.371/m
$a_{\text{particles}}$	665 nm	0.3565 \pm 0.20/m
a_{cdom}		0.173 \pm 0.04/m
a_{water}^a		0.281/m
$a_{\text{particles}}$	620 nm	0.287 \pm 0.05/m
a_{cdom}		0.273 \pm 0.07/m

^a Values for the absorption of water were taken from (Buiteveld et al., 1994).

C-PC concentrations from QuickBird radiance data was dependent entirely upon covariance between C-PC concentration with one or more measured surrogates. In this context, C-PC concentrations were best modeled using the first two principal components ($R^2 = 0.68$). WHO guidelines (WHO, 2003) for identifying areas potentially at risk, however, are not based on C-PC concentrations, but on Chl-*a* concentrations. Confirmation of that risk requires field observations to identify the presence and concentration of cyanotoxins. The spatial context provided by the predicted Chl-*a* and C-PC concentrations, is therefore of significant value to guide those sampling efforts.

QuickBird pigment mapping

The NIR/Red regression model was applied to the QuickBird radiance data to map predicted Chl-*a* concentrations across Missisquoi Bay (Fig. 4a). Predicted C-PC concentrations were mapped using the two-component PCA regression model.

As is shown in Fig. 4a, predicted Chl-*a* concentrations across much of the bay ranged from 60 to over 120 $\mu\text{g/L}$, with the highest concentrations located along the western and northern shorelines, in the southeast near where the Rock River enters Missisquoi Bay, and near the entrance to the bay along the south shore. Chl-*a* concentrations in excess of 120 $\mu\text{g/L}$ were also predicted along the frontal boundaries between the incoming Missisquoi River and bay waters. The lowest predicted Chl-*a* concentrations were located to the north and east of the Missisquoi River delta.

Predicted C-PC concentrations across the bay were consistent with cyanobacterial-dominated waters, yielding C-PC:Chl-*a* ratios ranging from 0.8 to 2.0 in most areas. Areas with highest predicted C-PC concentration coincided spatially with areas of highest predicted Chl-*a* concentration, with two notable exceptions. Predicted C-PC:Chl-*a* ratios for waters in the northwestern embayment (Baie de Venise)

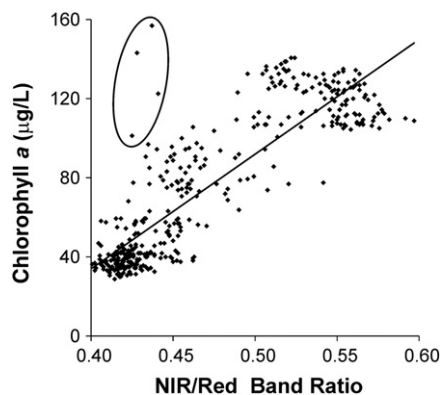


Fig. 3. QuickBird-derived NIR/Red band ratios versus measured chlorophyll *a* concentrations ($\mu\text{g/L}$) for Missisquoi Bay. The data points (circled) were the result of a temporal offset between the field and image data. The line shown represents the least squares linear regression model fit.

Table 4
Summary of regression results between QuickBird radiance and observed pigment concentrations ($\mu\text{g/L}$) ($n = 382$) along an east–west transect in Missisquoi Bay, August 17, 2004. Parameters in bold font were used to classify the QuickBird imagery.

QuickBird Spectral Bands			QuickBird PCA		
Dependent Variable	Independent Variable(s)	R^2	Dependent Variable	Independent Variable(s)	R^2
Chlorophyll <i>a</i>	Blue	0.26	Chlorophyll <i>a</i>	PC1	0.50
	Green	0.52		PC2	0.74
	Red	0.41		PC1-2	0.75
	NIR	0.74			
	NIR/red	0.75			
	(Blue-red)/green	0.48			
Phycocyanin	Blue	0.40	Phycocyanin	PC1	0.56
	Green	0.60		PC2	0.13
	Red	0.59		PC1-2	0.68
	NIR	0.23			
	NIR/red	0.09			
	(Blue-red)/Green	0.59			

and along the southeastern shoreline (Goose Bay) ranged between 0.35 and 0.5.

To set the context of these observations, World Health Organization (WHO) guidelines for a moderate health alert in recreational waters in which cyanobacteria are dominant is approximately 50 $\mu\text{g/L}$ of Chl-*a*, because at these cell densities cyanotoxins may reach concentrations with potential health impact (Chorus and Bartram, 1999; Hunter et al., 2009). It also marks the density at which *Microcystis* and *Anabaena* populations, in particular, may begin to form surface scums, within which cell densities and cyanotoxin concentrations may rapidly increase to greatly elevate the risk.

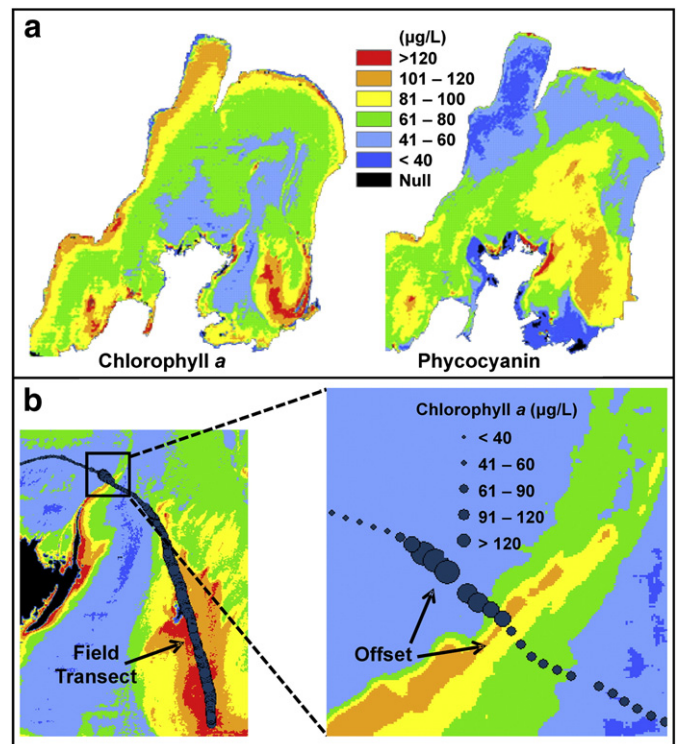


Fig. 4. (a) Predicted chlorophyll *a* and phycocyanin concentrations ($\mu\text{g/L}$) for Missisquoi Bay derived from QuickBird satellite imagery acquired 17 August, 2004. (b) Detail showing the spatial offset between the field measured and QuickBird-derived chlorophyll *a* concentrations near the Missisquoi River delta. Observations along the field transect were made within ± 1 h of the image acquisition. Winds were from the SSW at 14 km/h.

Registration accuracy

Fig. 4b shows a detailed view of predicted Chl-*a* concentrations near the mouth of the Missisquoi River with the corresponding georeferenced transect data overlain. On first look the spatial patterns observed in the two data sets appear to agree well. Closer examination of the pigment concentrations along the frontal boundary between the incoming Missisquoi River and bay waters, however, reveals a ~120 m spatial offset in the transect data relative to the QuickBird imagery. A similar front on the western edge of the incoming waters (data not shown) exhibited an 80 m offset in the same direction consistent with the prevailing winds.

In the context of most aquatic studies, an offset of 80–120 m between the imagery and calibration data might not impact the analysis, particularly when working with coarse spatial resolution data. The offset observations shown in Fig. 4b, however, are also identified in Fig. 3 as the outlying data points in the regression analysis used to calibrate the radiance data. Upon removing these observations from the analysis, the variability in Chl-*a* concentration explained by the NIR/Red regression model increased from 75 to 80%, but had little effect on the model coefficients. The potential of spatial offsets to dramatically affect modeling results, however, graphically demonstrates the need to acquire as near coincident field observations as possible when working with high spatial resolution imagery.

MERIS analyses

Chl-*a* concentrations retrieved from the August 24th and September 3rd MERIS spectral data are shown in Fig. 5. On August 24th, Chl-*a* concentrations ranging from 60 to ≥ 100 $\mu\text{g/L}$ were observed throughout much of Missisquoi Bay. Again, the highest concentrations were centered along the eastern shoreline and near the entrance to the bay, although the areal extent of the highest cell densities was markedly greater than observed the previous week. The lowest concentrations were observed east of the extensive Missisquoi delta wetlands. Observations on September 3rd, in contrast, indicated that the algal bloom that had dominated the bay in mid-to-late August had largely collapsed. Observed Chl-*a* concentrations throughout much of the bay at this time ranged from less than 20 to 40 $\mu\text{g/L}$. Concentrations exceeding 60 $\mu\text{g/L}$ were observed only along the western and northern shorelines.

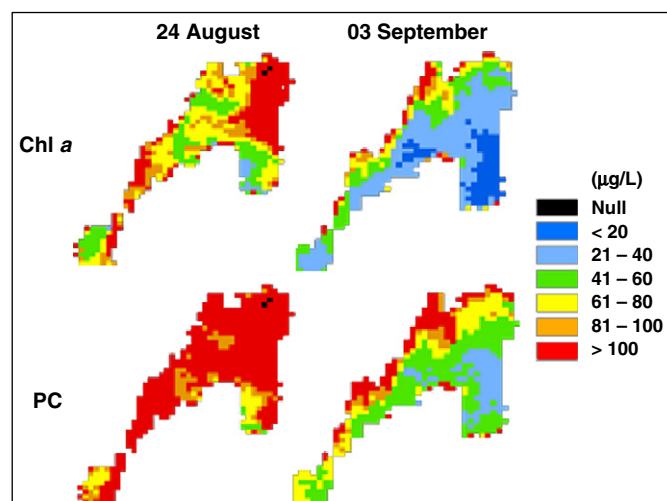


Fig. 5. MERIS-derived chlorophyll *a* and phycocyanin concentrations ($\mu\text{g/L}$) within Missisquoi Bay on August 24 and September 03, 2004.

C-PC concentrations exceeding 100 $\mu\text{g/L}$ were observed across most of the bay on August 24th, confirming cyanobacterial dominance of the phytoplankton community. Only in the incoming waters from the Missisquoi delta wetlands were observed C-PC concentrations notably lower. By September 3rd, however, C-PC concentrations across much of the bay had dropped below 60 $\mu\text{g/L}$, confirming the collapse of the August bloom. High C-PC concentrations (> 100 $\mu\text{g/L}$) along the western and northern shorelines marked the continued presence of dense localized cyanobacterial blooms adjacent these populated areas.

Validation

Chl-*a* concentrations retrieved from the MERIS spectral data agreed well with coincident transect observations made on August 24th and September 3rd aggregated to the same spatial resolution (MRE = -0.6% , $n = 17$; Fig. 6a). The limited variability in our observations points to the need for longer transects collected over a season to represent a wider range of conditions. Retrieved C-PC concentrations, in contrast, underestimated field measured concentrations in proportion to the actual concentrations (Fig. 6b). For example, whereas over the range of the concentrations observed, the mean residual error was only -2.1% , at C-PC concentrations greater than 80 $\mu\text{g/L}$ relative errors increased to between -10 and -20% . Confounding these results, however, is that the higher cell densities were also accompanied by an increase in the fraction of eukaryotic algae in the phytoplankton community (Table 2).

Discussion

In the absence of immediately available information on the presence or concentration of cyanotoxins, Chl-*a* is widely accepted as a surrogate measure of cyanobacterial density and, in turn, of the potential public health risk posed by cyanobacterial blooms. Conventional field sampling programs intending to assess this risk are dependent upon such measures, although they are typically severely limited in their ability to represent the spatially and temporally variable cyanobacterial populations. Remote sensing, as was demonstrated in this and other studies (Hunter et al., 2009), offers the potential to provide synoptic and timely information on the abundance and spatial distribution of cyanobacterial populations to facilitate preliminary risk assessment and ecological modeling efforts.

In this study, C-PC and Chl-*a* concentrations in the eutrophic waters of Missisquoi Bay, Lake Champlain were accurately retrieved from water-leaving radiance data as measured by Envisat's MERIS. Chl-*a* accuracies were high over the range of the concentrations observed. C-PC accuracies, in contrast, decreased as the fraction of cyanobacteria in the phytoplankton assemblage decreased and as population densities increased. Both factors are recognized as potential sources of error. Absorption by Chl-*a* and accessory pigments other than C-PC near the C-PC absorption maximum (620 nm) that is not accounted for by the Simis retrieval algorithm can lead to underestimation of C-PC concentration (Simis et al., 2005; Simis et al., 2007). Elevated NIR reflectance from high cell densities concentrated near or at the surface, e.g. surface scums, is also known to interfere with atmospheric correction algorithms which can lead to an underestimation of water-leaving radiance (Kutser, 2004; Moses et al., 2009). Underestimation of C-PC at higher cell densities may also result because current retrieval algorithms cannot account for variable pigment absorption efficiencies, i.e. the recognized non-linear relationship between C-PC concentration and energy absorption at 620 nm (Reinart and Kutser, 2006). Pigment absorption efficiencies, in turn, may vary as a function of season, nutrient or light availability, and phytoplankton community composition (Gitelson et al., 2000). Nonetheless, the relatively high accuracies observed in estimating pigment concentrations attests to the value of the MERIS data and the robustness of the semi-analytical retrieval algorithms to quantify cyanobacterial

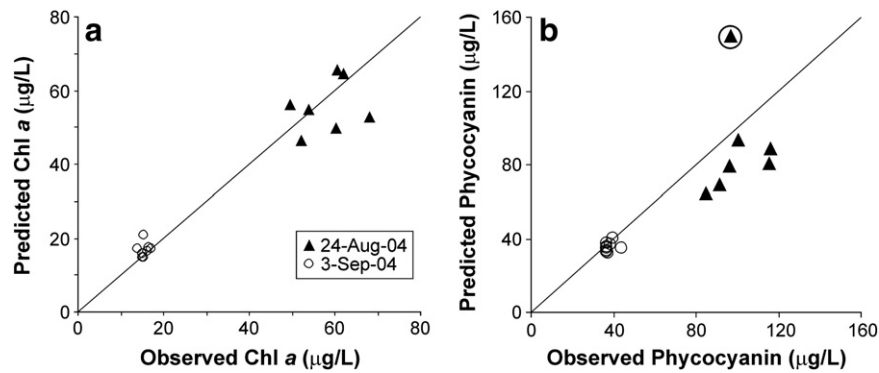


Fig. 6. MERIS-predicted versus field measured (a) chlorophyll *a* concentrations ($n = 17$) and (b) phycocyanin concentrations ($n = 16$) for Missisquoi Bay. The reference line shown represents a 1:1 correspondence between the predicted and observed values. The outlying datum circled was not included in the analyses.

cell densities over the range of concentrations that pose a significant risk to human health.

The relatively coarse spatial resolution (300 m) MERIS data were also compared with pigment concentrations predicted from empirically-calibrated high spatial resolution (2.4 m) QuickBird imagery. The spatial detail inherent in the high spatial resolution imagery allowed the identification of fine-scaled features and their spatial relationships that could prove of significant value in studies of cyanobacterial bloom formation and propagation in inland waters. The spatial structure evident in the concentration data derived from both the low and high spatial resolution imagery, however, confirmed the potential value of either to support preliminary health risk assessments posed by cyanobacteria blooms, aid understanding of bloom dynamics, and direct follow-on sampling efforts.

Our analyses over a 17 day period captured the peak and collapse of a late summer cyanobacterial bloom, illustrating the spatial complexity and dynamics of cyanobacterial distributions within Missisquoi Bay. Chl-*a* and C-PC concentrations derived from the August 17th (QuickBird) and August 24th (MERIS) imagery indicated that cyanobacterial densities across much of the bay posed a moderate to high risk to animal and human health, based on provisional WHO guidelines (WHO, 2003). Concentrations retrieved from September 3rd MERIS imagery, in contrast, indicated that the blooms had largely collapsed, except along the northwestern shoreline where cell densities still posed a significant risk to adjacent populated areas.

In sharp contrast, authorities tasked with assessing the health risks of potentially toxic cyanobacterial blooms in Missisquoi Bay failed to detect this bloom event altogether. The Chl-*a* concentration from a single bi-weekly observation taken August 24th intended to represent Missisquoi Bay as a whole was $1.8 \mu\text{g/L}$ (VTDEC, 2010), far below the WHO monitoring guidelines (WHO, 2003) required to trigger further action. In comparison, Chl-*a* and C-PC concentrations retrieved from the MERIS imagery on the same date indicated a dense cyanobacterial bloom (60 to $>100 \mu\text{g/L}$ Chl-*a*) was present across much of the bay. Had our observations been part of the monitoring effort, it would have prompted follow-on field observations to determine the presence, type and concentration of cyanotoxins, and alerting shoreline communities of potential risk to recreational users and drinking water sources.

This example highlights not only the fragmentary insight that conventional point sampling efforts provide in determining the potential public health risk of cyanobacterial blooms, but also the need to recognize that the statistical confidence provided by synoptic remote sensing observations greatly exceeds that possible using conventional sampling approaches based on a limited number of observations.

In application, remote sensing should be viewed as one component of an integrated monitoring system supporting prelim-

inary risk assessment activities. Spatial and temporal variability in the toxicity of cyanobacterial blooms, however, will require subsequent field sampling to assess the presence, type and concentration of cyanotoxins (Hunter et al., 2009). Unlike with conventional water sampling approaches, the spatial context provided by the mapped pigment concentration and preliminary risk assessment data can also be used to direct follow-on sampling efforts, thereby improving the cost effectiveness of the field sampling effort, or to focus assessments on prioritized areas of concern to improve risk management. Periodic validation of the retrieval algorithms will also be required to gain further insight into the performance of the retrieval algorithms under different phases of bloom formation and senescence, phytoplankton community composition, and over a wide range of cell densities.

At present, Envisat's MERIS is the only spaceborne sensor with a spectral configuration that will allow Chl-*a* and C-PC concentrations to be retrieved directly from the radiance data without the aid of coincident field observations. The relatively coarse spatial resolution (300 m) of this sensor, however, limits its application to moderate-to-large inland waters. Continued improvements in the atmospheric correction and retrieval algorithms applicable to MERIS will only strengthen the value of this sensor in monitoring programs for which it is suited.

Integration of remote sensing into monitoring efforts for smaller waters must await the development of new satellite sensors with the appropriate spatial resolution and spectral configuration. The German-led hyperspectral, medium spatial resolution (~ 30 m) Environmental Mapping and Analysis Program (EnMAP) satellite system, scheduled for launch in 2014 is designed for this purpose (Stuffer et al., 2009). The use of airborne hyperspectral sensors or imaging spectrometers with the spectral and spatial capabilities required to monitor cyanobacteria blooms in small to moderate-sized inland waters would also offer the advantages of flexible scheduling and reduced atmospheric attenuation.

Conclusion

The ability to use radiance measures to accurately quantify phycocyanin and chlorophyll-*a* concentrations as indicators of cyanobacteria cell density in eutrophic waters without the need for coincident field observations was demonstrated in Missisquoi Bay, Lake Champlain. The 300 m spatial resolution, spectral configuration, and 2–4 day revisit capability of Envisat's MERIS, in combination with atmospheric correction and semi-analytical retrieval algorithms, make this approach well suited to support timely assessments of the public health risks posed by cyanobacterial blooms in these waters. Viewed as one component of an integrated monitoring approach, the synoptic spatial and multi-temporal information provided by remote sensing affords water quality and public health management the opportunity to

significantly improve public health risk assessment associated with cyanobacterial blooms.

Acknowledgments

Funding for this research was provided by the U.S. Geological Survey through the Vermont Center for Water Resources and Lake Studies. MERIS data were provided by the European Space Agency. We extend our thanks to Stefan Simis, Antonio Ruiz-Verdú, and Antonio Quesada for their helpful advice in the early phase of this project. We also wish to thank the anonymous reviewers whose comments contributed substantially to improving an earlier draft of this manuscript.

References

- Becker, R.J., Sultan, M.I., Boyer, G.L., Twiss, M.R., Konopko, E., 2009. Mapping cyanobacteria blooms in the Great Lakes using MODIS. *J. Great Lakes Res.* 35, 447–453.
- Brando, V.E., Dekker, A.G., 2003. Satellite hyperspectral remote sensing for estimating estuarine and coastal water quality. *IEEE Trans. Geosci. Remote. Sens.* 41, 1378–1387.
- Chacon-Torres, A., Ross, L.G., Beveridge, M.C.M., Watson, A.I., 1992. The application of SPOT multispectral imagery for the assessment of water-quality in Lake Patzcuaro, Mexico. *Int. J. Remote Sens.* 13, 587–603.
- Chang, K.W., Shen, Y., Chen, P.C., 2004. Predicting algal bloom in the Teché reservoir using Landsat TM data. *Int. J. Remote. Sens.* 25, 3411–3422.
- Chorus, I., Bartram, J., 1999. *Toxic Cyanobacteria in Water: A Guide to their Public Health Consequences, Monitoring and Management*. E & FN Spon, London, England.
- Dekker, A.G., Malthus, T.J., Wijnen, M.M., Seyhan, E., 1992. Remote sensing as a tool for assessing water quality in Loosdrecht lakes. *Hydrobiologia* 233, 137–159.
- Doerffer, R., Schiller, H., 2007. The MERIS case 2 water algorithm. *Int. J. Remote. Sens.* 23, 517–535.
- Downing, J.A., Watson, S.B., McCauley, E., 2001. Predicting cyanobacteria dominance in lakes. *Canadian Journal of Fisheries and Aquatic Science* 58, 1905–1908.
- ESRI, 2010. ArcGIS. <http://www.esri.com/ESR>.
- Falconer, I.R., 2001. Toxic cyanobacterial bloom problems in Australian waters: risks and impacts on human health. *Phycologia* 40, 228–233.
- Fomferra, N., Brockmann, C., 2006. The BEAM Project. Carsten Brockmann Consult, Hamburg, Germany.
- Gitelson, A.A., Yacobi, Y.Z., Schalles, J.F., Rundquist, D.C., Han, L., Stark, R., Etzion, D., 2000. Remote estimation of phytoplankton density in productive waters. *Archives for Hydrobiologia - Special Issues Advancements in Limnology* 55, 121–136.
- Gons, H.J., Auer, M.T., Effler, S.W., 2008. MERIS satellite chlorophyll mapping of oligotrophic and eutrophic waters in the Laurentian Great Lakes. *Remote. Sens. Environ.* 112, 4098–4106.
- Gons, H.J., Rijkeboer, M., Ruddick, K., 2002. A chlorophyll-retrieval algorithm for satellite imagery (Medium Resolution Imaging Spectrometer) of inland and coastal waters. *J. Plankton Res.* 24, 947–951.
- Gons, H.J., Rijkeboer, M., Ruddick, K.G., 2005. Effect of a waveband shift on chlorophyll retrieval from MERIS imagery of inland and coastal waters. *J. Plankton Res.* 27, 125–127.
- Hunter, P.D., Tyler, A.N., Carvalho, L., Codd, G., Maberly, S.C., 2010. Hyperspectral remote sensing of cyanobacterial pigments as indicators for cell populations and toxins in eutrophic lakes. *Remote. Sens. Environ.* 114, 2705–2718.
- Hunter, P.D., Tyler, A.N., Gilvear, D.J., Willby, N.L., 2009. Using remote sensing to aid the assessment of human health risks from blooms of potentially toxic cyanobacteria. *Environ. Sci. Technol.* 43, 2627–2633.
- Hunter, P.D., Tyler, A.N., Presing, M., Kovacs, A.W., Preston, T., 2008a. Spectral discrimination of phytoplankton colour groups: the effect of suspended particulate matter and sensor spectral resolution. *Remote. Sens. Environ.* 112, 1527–1544.
- Hunter, P.D., Tyler, A.N., Willby, N.J., Gilvear, D.J., Hunter, P.D., Tyler, A.N., Willby, N.J., Gilvear, D.J., 2008b. The spatial dynamics of vertical migration by *Microcystis aeruginosa* in a eutrophic shallow lake: a case study using high spatial resolution time series airborne remote sensing. *Limnol. Oceanogr.* 53, 2391–2406.
- Jupp, D., Kirk, J., Harris, G.P., 1994. Detection, identification and mapping of cyanobacteria — using remote sensing to measure the optical quality of turbid inland waters. *Australian Journal of Marine and Freshwater Research* 45, 801–828.
- Koponen, S., Pulliainen, J., Servomaa, H., Zhang, Y., Hallikainen, M., Kallio, K., Vepsäläinen, J., Pyhalhti, T., Hannonen, T., 2001. Analysis on the feasibility of multi-source remote sensing observations for Chl-a monitoring in Finnish lakes. *Sci. Total. Environ.* 268, 95–106.
- Krause, K., 2003. Radiance conversion of QuickBird data. DigitalGlobe Technical Note 2003-07-07DigitalGlobe, Inc.
- Kutser, T., 2004. Quantitative detection of chlorophyll in cyanobacterial blooms by satellite remote sensing. *Limnol. Oceanogr.* 49, 2179–2189.
- Kutser, T., Metasamaa, L., Strombeck, N., Vahtmae, E., 2006. Monitoring cyanobacteria blooms by satellite remote sensing. *Estuar. Coast. Shelf Sci.* 67, 303–312.
- LCBP, 2002. Missisquoi Bay Agreement. <http://www.lcbp.org/missisquoi.htm>.
- LCBP, 2010. Opportunities for Action: An Evolving Plan for the Future of the Lake Champlain Basin. <http://www.lcbp.org/PDFs/OpportunitiesForAction2010.pdf>.
- Leica, Geosystems, 2009. ERDAS Imagine 9.3.
- Matthews, M., Bernard, S., Winter, K., 2010. Remote sensing of cyanobacteria-dominant algal blooms and water quality parameters in Zeekoovleij, a small hypertrophic lake, using MERIS. *Remote. Sens. Environ.* 114, 2070–2087.
- Mayo, M., Gitelson, A., Yacobi, Y.Z., Ben-Avraham, Z., 1995. Chlorophyll distribution in Lake Kinneret determined from Landsat Thematic Mapper data. *Int. J. Remote. Sens.* 16, 175–182.
- Mihuc, T.B., Boyer, G.L., Jones, J., Satchwell, M.F., Watzin, M., 2006. Lake Champlain phytoplankton and algal toxins: present and past. *Great Lakes Res. Rev.* 7, 18–21.
- Mihuc, T.B., Boyer, G.L., Satchwell, M.F., Pellam, M., Jones, J., Vasile, J., Bouchard, A., Bonham, R.E., 2005. Phytoplankton community composition and cyanobacterial toxins in Lake Champlain, U.S.A. *Verh. Internat. Verein. Limnol.* 29, 328–333.
- Mihuc, T.B., Pershyn, C., Thomas, S., Boyer, G.L., Satchwell, M.F., Jones, J., Allen, E., Greene, M., 2008. Cyanobacteria and the sixth Great Lake: community dynamics of toxic algal blooms in Lake Champlain, USA. *Verh. Internat. Verein. Limnol.* 30, 312–317.
- Missisquoi Bay Inter-Agency Advisory Committee—Montérégie, 2004. Missisquoi Bay Phosphorus Reduction Action Plan 2003–2009.
- Moses, W.J., Gitelson, A., Bernikov, S., Povazhnyy, V., 2009. Estimation of chlorophyll-*a* concentration in case II waters using MODIS and MERIS data —successes and challenges. *Environ. Res. Lett.* 4, 045005.
- Pan, X., Mannino, A., Russ, M.E., Hooker, S.B., Harding Jr., L.W., 2010. Remote sensing of phytoplankton pigment distribution in the United States northeast coast. *Remote. Sens. Environ.* 114, 2403–2416.
- Pierson, D.C., Strombeck, N., 2001. Estimation of radiance reflectance and the concentrations of optically active substances in Lake Malaren, Sweden, based on direct and inverse solutions of a simple model. *Sci. Total. Environ.* 268, 171–188.
- Quesada, A., Vincent, W.F., 1999. Community and pigment structure of Arctic cyanobacterial assemblages: the occurrence and distribution of UV absorbing compounds. *FEMS Microbiol. Ecol.* 28, 315–323.
- Rahman, H., Dedieu, G., 1994. A simplified method for the atmospheric correction of satellite measurements in the solar spectrum. *Int. J. Remote. Sens.* 15, 123–143.
- Rantajarvi, E.R., Olsonene, R., Hallfors, S., Leppanen, J., Raateoja, M., 1998. Effect of sampling frequency on detection of natural variability in phytoplankton: unattended high-frequency measurements on board ferries in the Baltic Sea. *ICES J. Mar. Sci.* 55, 697–704.
- Reinart, A., Kutser, T., 2006. Comparison of different satellite sensors in detecting cyanobacterial bloom events in the Baltic Sea. *Remote. Sens. Environ.* 102, 74–85.
- Reynolds, C.S., 1984. *The Ecology of Freshwater Phytoplankton*. Cambridge Univ. Press, Cambridge and New York.
- Ruiz-Verdú, A., Simis, S.G.H., de Hoyos, C., Gons, H.J., Peña-Martínez, R., 2008. An evaluation of algorithms for the remote sensing of cyanobacterial biomass. *Remote. Sens. Environ.* 112, 3996–4008.
- Sartory, D.P., Grobbelaar, J.U., 1984. Extraction of chlorophyll *a* from freshwater phytoplankton for spectrophotometric analysis. *Hydrobiologia* 114, 177–187.
- SAS, 2010. SAS 9.2 Software. SAS Institute Inc.
- Schroeder, T., Behnert, I., Schaale, M., Fischer, J., Doerffer, R., 2007. Atmospheric correction algorithm for MERIS above case-2 waters. *Int. J. Remote. Sens.* 28, 1469–1486.
- Simis, S.G.H., Peters, S.W.M., Gons, H.J., 2005. Remote sensing of the cyanobacterial pigment phycocyanin in turbid inland water. *Limnol. Oceanogr.* 50, 237–245.
- Simis, S.G.H., Ruiz-Verdú, A., Dominguez-Gómez, J.A., Peña-Martínez, R., Peters, S.W.M., Gons, H.J., 2007. Influence of phytoplankton pigment composition on remote sensing of cyanobacterial biomass. *Remote. Sens. Environ.* 106, 414–427.
- Smeltzer, E., 2003. *The Phosphorous Problem in St. Albans Bay: A Summary of Research Findings*. Vermont Department of Environmental Conservation, Waterbury, Vermont, USA.
- Stuffer, T., Forster, K., Hofer, S., Leipold, M., Sang, B., Kaufmann, H., Penne, B., Mueller, A., Chlebek, C., 2009. Hyperspectral imaging — an advanced instrument concept for the EnMAP mission (environmental mapping and analysis programme). *Acta Astronaut.* 65, 1107–1112.
- Torbick, N., Hu, F., Zhang, J., Qi, J., Zhang, H., Becker, B., 2008. Mapping Chlorophyll-*a* concentrations in West Lake, China using Landsat 7 ETM+. *J. Great Lakes Res.* 34, 559–565.
- U.S. EPA, 2002. Lake Champlain Phosphorus Total Maximum Daily Load. <http://www.lcbp.org/tmdl.htm>.
- Vincent, R.K., Qin, X., McKay, M.L., Miner, J., Czajkowski, K., Savino, J., Bridgeman, T., 2004. Phycocyanin detection from LANDSAT data for mapping cyanobacterial blooms in Lake Erie. *Remote. Sens. Environ.* 89, 381–392.
- Vincent, W.F., 2009. Cyanobacteria. In: Likens, G.E. (Ed.), *Encyclopedia of Inland Waters*. Elsevier, Oxford, UK, pp. 226–232.
- VTDEC, 2010. Lake Champlain Long Term Monitoring. Vermont Department of Environmental Conservation. http://www.vtwaterquality.org/cfm/champlain/lp_longterm-lakes.cfm.
- Watzin, M.C., Miller, E.B., Shambaugh, A.D., Kreider, M.A., 2006. A partnership approach to monitoring cyanobacteria in Lake Champlain. *Great Lakes Res. Rev.* 7, 8–13.
- WHO, 2003. *Coastal and Fresh Waters. Guidelines for Safe Recreational Water Environments*, Vol. 1. World Health Organization, Geneva.
- Wyman, M., Fay, P., 1986. Underwater light climate and the growth and pigmentation of planktonic blue-green algae (cyanobacteria) I. The influence of light quantity. *Proceedings of the Royal Society of London. Series B. Biological Sciences* 227, 367–380.
- Yacobi, Y.Z., Gitelson, A., Mayo, M., 1995. Remote sensing of chlorophyll in Lake Kinneret using high-spectral-resolution radiometer and Landsat TM- spectral features of reflectance and algorithm development. *J. Plankton Res.* 17, 2155–2173.